Light Metals 2011 *Edited by: Stephen J. Lindsay*
TMS (The Minerals, Metals & Materials Society), 2011

Study on solution of Al_2O_3 in low temperature aluminum electrolyte

Hongmin Kan[1], Ning Zhang[1], Xiaoyang Wang[1]

[1]Key Laboratory of Advanced Materials Technology of Liaoning province, Shenyang University, Shenyang 110044, China

Keywords: Low temperature aluminum electrolyte, Alumina, Image analysis

Abstract

Current efficiency can be increased and energy consumption can be lowered by low temperature aluminum electrolysis. However, many problems will occur, such as low electrical conductivity, cathode shell, low alumina solubility and alumina-solution rates if the temperature is too low. Of these problems, low alumina solubility and alumina-solution rate are difficult problems. In this paper, a novel method that can measure the solubility and dissolution rate of Al_2O_3 is introduced based on early research. The double rooms' transparent quartz electrobath is used for low temperature aluminum electrolysis. The image sequence is obtained by taking from the double rooms' transparent quartz electrobath. Image analysis techniques are used to compute the change of solubility and dissolution rate of Al_2O_3. The method can analyze the influence factors of solubility and dissolution rate of Al_2O_3 intuitively and roundly by transparent quartz electrobath and image analysis techniques.

Introduction

Low temperature aluminium electrolysis has been one of active research fields in recent years [1-5]. Traditional Hall- Héroult electrolysis process for aluminium production usually operates at very high temperature (nowadays about 950℃) and unavoidably shows high energy consumption, complicated operation and emissions. By the introduction of low-melting baths one might expect an increase in current efficiency and lower energy consumption. It is important to reduce liquidus temperature for study on low temperature aluminium electrolysis. But many problems will occur, such as low electrical conductivity, cathode shell, and low alumina solubility and alumina-solution rates when the temperature is too low. These problems have seriously affected the application of low-temperature aluminum electrolysis in industry. In many problems, the single largest problem is the solubility of alumina.

An important indicator one determines the performance of alumina in electrolytic aluminum production is the solubility of alumina. When the temperature of aluminium electrolysis is lowered, low alumina solubility and alumina-solution rates cause alumina can not be completely dissolved or quickly dissolved in molten cryolite. Alumina will deposite on bottom, thus the physical and chemical processes and heat balance of the electrolysis cell are severely affected.

Many previous measurements of alumina solubility have been published and significant progress has been made [6-10]. The solubility of alumina in molten Na_3AlF_6 containing various amounts of AlF_3, CaF_2, and LiF was determined by measuring the weight loss of a rotating sintered corundum disc. The empirical expression was given. Welch [10] et al. studied crust and alumina powder dissolution in aluminum smelting electrolytes. Yushu [7] measured the solubility of Al_2O_3 in basic cryolite melts experimentally for $3 \leq$cryolite ratio $r \leq 12.5$ at 1300K. Gerlach [6] studied the dissolution of aluminum oxide in cryolite melts. Al_2O_3 samples pressed to tablets were dissolved in cryolite melts. They discovered that the dissolution rate changed at an Al_2O_3 content of 5 to 6 pct in the cryolite melts. Qiu[4] et al. developed transparent quartz electrobath in1985. Dissolution behavior of alumina can be observed more intuitively and roundly by transparent quartz electrobath. In recent years, research group studied the dissolution behavior of alumina in molten cryolite by transparent quartz electrobath and photographed the whole process of dissolution of alumina with a video. Research group analyzed and discussed some of the impact factors of dissolution of alumina [11-15].

In this paper, a novel method that can measure the solubility and dissolution rate of Al_2O_3 is introduced based on early research. The double rooms' transparent quartz electrobath is used for low temperature aluminum electrolysis. The image sequence is obtained by taking from the double rooms' transparent quartz electrobath. Image analysis techniques are used to compute the change of solubility and dissolution rate of Al_2O_3. The method can analyze the influence factors of solubility and dissolution rate of Al_2O_3 intuitively and roundly by transparent quartz electrobath and image analysis techniques.

Computing dissolution rate of Al_2O_3 based on image sequence analysis

Factors and constraints

Here the double rooms' transparent quartz electrobath is used for a container. Alumina powder is added into the transparent quartz electrobath. Factors of dissolution rate of Al_2O_3 are considered. Then constraints which the following algorithm will use are set. These factors are temperature of the transparent quartz electrobath, quality of Al_2O_3, rate in which Al_2O_3 is added, stirring, additives used, composition ratio of additives. Although capacity of the transparent quartz electrobath does not affect shape of dissolution rate varying curve of Al_2O_3, it does affect the critical value of dissolution rate varying curve of Al_2O_3. Suppose that $V_{transelectrolyzer}$ denotes capacity of the transparent quartz electrobath, $T_{transelectrolyzer}$ denotes temperature of the transparent quartz electrobath, $Q_{alumina}$ denotes quality of Al_2O_3, $V_{alumina}$ denotes rate of which Al_2O_3 is added, T_{stir} denotes times of stirring, V_{stir} denotes speed of stirring, $V_{additive}$ denotes additives used, $P_{additive}$ denotes composition ratio of additives, then the factor set affecting dissolution rate of Al_2O_3 $S_{dissoluationrate}$ can be denoted as

$$S_{dissolutionrate} = \{V_{transelectrolyzer}, T_{transelectrolyzer}, Q_{alumina}, V_{alumina}, \quad (1)$$

T_{stir}, V_{stir}, $V_{additive}$, $P_{additive}$}

In the paper, the method that computes the dissolution rate of Al_2O_3 is proposed based on image sequence analysis. Each element is set in the factor set $S_{dissolutionrate}$. Image analysis and understanding is used for image sequence of Al_2O_3 which is taken from the transparent quartz electrobath. The dissolution rate varying curve of Al_2O_3 is developed. Then the dissolution rate varying equation of Al_2O_3 is devloped. Here the constraints for $S_{dissolutionrate}$ are set as followed. Suppose $V_{transelectrolyzer}$=a, $T_{transelectrolyzer}$=b, $Q_{alumina}$=c, $V_{alumina}$=d, T_{stir}=e, V_{stir}=f, $V_{additive}$=g, $P_{additive}$=h, then dissolution rate of Al_2O_3 $DV_{alumina}$ can be denoted as:

$$DV_{alumina} = DV((V_{transelectrolyzer}=a)\cdot(T_{transelectrolyzer}=b)\cdot(Q_{alumina}=c)\cdot(V_{alumina}=d)\cdot(T_{stir}=e)\cdot(V_{stir}=f)\cdot(V_{additive}=g)\cdot(P_{additive}=h)) \quad (2)$$

Here, DV denotes dissolution rate function, operator "·" denotes dependence relation among constraints.

It should be noticed that the factor set $S_{dissolutionrate}$ can be extended dynamically and parameter value can be changed dynamically. This makes it possible that constraints can be changed by application.

Algorithm computing dissolution rate of Al_2O_3

Here the image sequence of Al_2O_3 dissolution is taken from the transparent quartz electrobath. It can be found that each image contains a large amount of texture information. Our idea is as follows: First, the image sequence of Al_2O_3 dissolution is taken at a specific time interval. The image sequence is regarded as a point set where each point corresponds to an image at a specific time. Texture features of each image are used to characterize a point. Then, the similarity between neighboring points is used to describe dissolution rate variation of Al_2O_3, so that the dissolution rate varying curve of Al_2O_3 can be drawn. Then, approximation and interpolation techniques are used to establish the dissolution rate varying equation of Al_2O_3. Finally, dissolution rate of Al_2O_3 can be computed by the equation. The flowchart by which dissolution rate of Al_2O_3 can be computed based on image sequence analysis can refer to Fig.1. The error of the method is caused mainly by sampling time of one time and time interval of sampling.

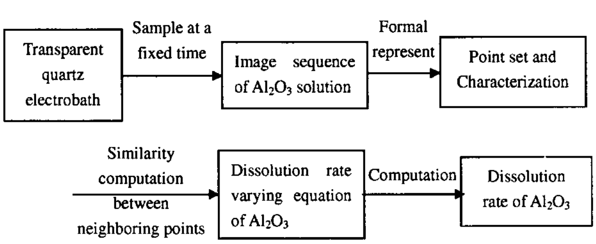

Fig.1 Flowchart for computing the dissolution rate of Al_2O_3 based on image sequence analysis

Computing information region in Al_2O_3 dissolution image

Here image sequence of Al_2O_3 dissolution is taken from the transparent quartz electrobath at a fixed time interval. Then information region is computed in each image. It can be found in Fig.2 that Al_2O_3 dissolution image contain three regions: *information region* (Al_2O_3 dissolution region, Fig.2(a)), *interference region* (Transparent quartz electrobath region, Fig.2(b)) and *background region* (Black region, Fig.2(c)). As far as Computation of Al_2O_3 dissolution rate is concerned, the information region is most important. Here rectangle window, such as A and B, is used to compute the information region.

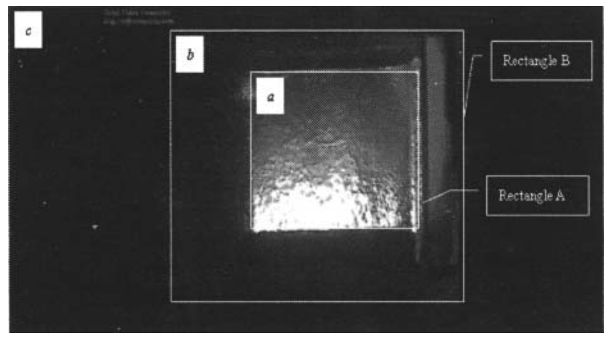

Fig.2 Al_2O_3 dissolution image (a)information region (b)interference region (c)background region

When Al_2O_3 dissolution images are taken, the position of camera and distance from camera to the transparent quartz electrobath is relatively fixed. This means that the position and scale of a rectangle window can be decided in advance. Here the point at the upper left corner is selected as a reference point. The scale of rectangle window A is A1 × A2 and the position is (P1, P2). The scale of rectangle window B is B1 × B2 and the position is (P3, P4).

Suppose that $f(x, y)$ denotes an Al_2O_3 dissolution image of size M × N. The equation (3) can be used to decide whether a point (x, y) is in information region.

$$P1 <= x <= P1 + A1 \text{ and } P2 <= y <= P2+A2 \quad (3)$$

Here x = P1 and x = P1+A1 are left boundary and right boundary of the information region respectively, y = P2 and y = P2+A2 are upper boundary and bottom boundary respectively.

Extracting texture features from information region of Al_2O_3 dissolution image

It can be found in Fig.2(a) that the information region of the Al_2O_3 dissolution image contain a large amount of texture. Here texture features are used to characterize an image, and the co-occurrence matrix method is used to compute the texture features.

First, the image sequence is taken through the transparent quartz electrobath. Then, color images are transformed into gray images by gray-scale transformation. Suppose that $f(x, y)$ denotes gray image of Al_2O_3 dissolution. If N_g denotes gray scale of the image, then co-occurrence matrix can be denoted as:

$$P(i, j, d, \theta) = count\,\{((x_1, y_1), (x_2, y_2)) \mid (x_1, y_1) \in (L_r \times L_c), (x_2, y_2) \in (L_r \times L_c), \quad (4)$$

$(x_2, y_2) = (x_1, y_1) + (d \cos\theta, d \sin\theta), f(x_1, y_1) = i, f(x_2, y_2) = j, 0 \le i, j \le N_g\}$

Here *count* (·) is used to denote number of pixel pairs which is to satisfy the condition in the set. The parameter d denotes the distance between pixels. The parameter θ denotes the angle between line denoted by pixel pair and horizontal direction.

Five parameters, which are *angular second moment*, *contrast*, *correlation*, *inverse difference moment*, *entropy*, are computed according to the co-occurrence matrix $P(i, j, d, \theta)$. The five feature can be denote as:

$$Angular\ Second\ Moment = \sum_{i=0}^{N_g-1}\sum_{j=0}^{N_g-1} P^2(i,j) \quad (5)$$

$$Contrast = \sum_{n=0}^{N_g-1} n^2 (\sum_{i=0}^{N_g-1}\sum_{j=0}^{N_g-1} P(i,j)), \quad |i-j| = n \quad (6)$$

$$Correlation = \frac{1}{\delta_x \delta_y}\sum_{i=0}^{N_g-1}\sum_{j=0}^{N_g-1} ijP(i,j) - \mu_x \mu_y \quad (7)$$

$$Inverse\ Difference\ Moment = \sum_{i=0}^{N_g-1}\sum_{j=0}^{N_g-1} \frac{P(i,j)}{1+(i-j)^2} \quad (8)$$

$$Entropy = -\sum_{i=0}^{N_g-1}\sum_{j=0}^{N_g-1} P(i,j)\log(P(i,j)) \quad (9)$$

Here the parameters μ_x, μ_y, σ_x, σ_y denote mean and standard deviation of probability density function Px and Py, which can be denoted as

$$P_x(i) = \sum_{j=0}^{N_g-1} P(i,j) \qquad i = 0,1,\cdots,N_g - 1 \quad (10)$$

$$P_y(j) = \sum_{i=0}^{N_g-1} P(i,j) \qquad j = 0,1,\cdots,N_g - 1 \quad (11)$$

Here the d is set as 1, 3 and 5 respectively in equation (4). The values for θ is set as 0°, 45°, 90° and 135°, respectively. Then equation (4) is used to compute 12 co-occurrence matrices. Then the five features are computed from 12 co-occurrence matrices, and texture feature vector consists of these features.

Computation of dissolution rate equation of Al_2O_3

Here the dissolution rate equation of Al_2O_3 will be computed. After the image sequence of Al_2O_3 dissolution is obtained from the transparent quartz electrobath using a fixed time interval, the images can be regarded as an ordered point set. Furthermore, texture feature vectors can be used to characterize a point. Refer to Fig.3.

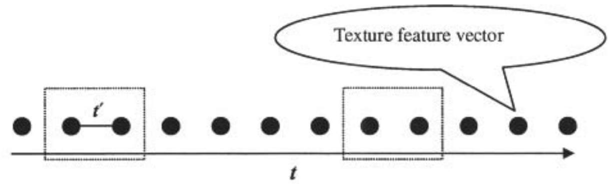

Fig.3 Image sequence of Al_2O_3 dissolution

Here t' which is sampling time of one time denotes time interval between points in the ordered point set. If t' is sufficiently small, then it can be assumed that the dissolution rate of Al_2O_3 can be changed at a fixed rate at t' time interval. Time interval between two samples is called as time interval of sampling. If time interval of sampling is too small then this will result in a large number of calculations. If time interval of sampling is too large then there is a risk that the rate of alumina dissolution changes within the selected interval of sampling.

Our approach is to use the similarity between texture feature vectors of two image points to describe dissolution rate variation of Al_2O_3. If t' is sufficiently small, then the dissolution rate of Al_2O_3 can be denoted as quotient between similarity and t'.

Suppose that Euclidean distance is used as similarity measure, then the similarity between texture feature vectors of two image points can be denoted as:

$$Similarity(T_{t1}, T_{t2}) = (\sum_{s=1}^{12}[T_{t1}(s) - T_{t2}(s)]^2)^{½} \quad (12)$$

Here T_{t1} and T_{t2} denote the texture feature vectors of two image points at t' time interval in the ordered point set respectively. The dissolution rate of Al_2O_3 $DV_{alumina}$ can be denoted as:

$$DV_{alu\min a} = \frac{Similarity(T_{t1}, T_{t2})}{t'} \quad (13)$$

Suppose that the image point set of Al_2O_3 dissolution consists of *num* elements. The *k* resampling is carried out for image sequence of Al_2O_3 dissolution in Fig.3. The information can be regarded as a sample in the dashed box. Then equations (12) and (13) are used to compute dissolution rate of Al_2O_3 so that the dissolution rate varying point set of Al_2O_3 can be developed. Then a polynomial approximation is used for the point set to compute dissolution rate varying equation of Al_2O_3. Finally, the dissolution rate of any time can be computed by initial value of dissolution rate and dissolution rate varying equation of Al_2O_3.

Experiments and analyses

In this paper, dissolution rate of alumina is studied. The electrolyte system is Na_3AlF_6-AlF_3-Al_2O_3-CaF_2-LiF-MgF_2. The liquidus temperature is about 900℃.

To compute the varying curves of dissolution rate about alumina in cryolite molten salt, a prototype system is designed by the above approach, and compiled by Java.

The configuration of computer for test is Intel(R) Celeron(R) mainboard, 1.60GHZ CPU main frequency, and 256 MB memory. Test result for alumina is shown in Fig.4.

The value in the first textbox is sampling time of one time, and described by the number of image points in sampling of one time. The result computed by the value minus 1 multiply sampling time of image sequence is t' in Fig.3. The value in the second textbox is time interval of sampling which refers to time interval between two sampling, and described by the number of image points.

Here the dissolution of alumina is sampled at a fixed time interval of one second.

When the value is 2 in the first textbox and the value is 3 in the second textbox, the dissolution rate varying curve is shown in Fig.4 for alumina.

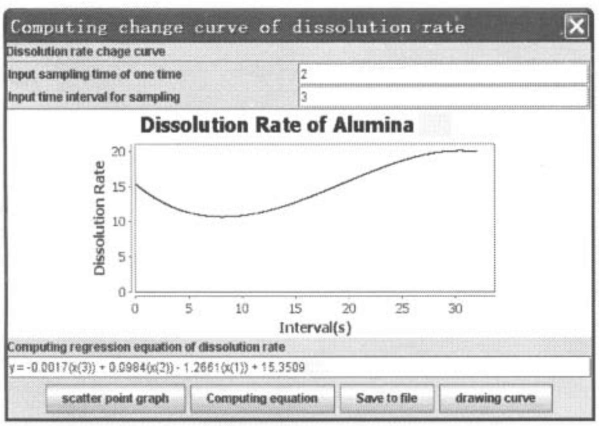

Fig. 4 Test results for alumina

The equation about the dissolution rate of alumina is

$$y_2 = -0.0017x^3+0.0984x^2-1.2661x+15.3509 \quad (15)$$

Here x denotes sample, y_1 is the dissolution rate of alumina at sample x which is computed by the method in the paper.

Conclusions

A novel method which can measure the solubility and dissolution rate of Al_2O_3 is introduced.

The method can analyze the influence factors of solubility and dissolution rate of Al_2O_3 intuitively and roundly by transparent quartz electrobath and image analysis techniques.

Image analysis techniques are used to compute the change of dissolution rate of Al_2O_3. The dissolution rate equation of alumina is established base on this method:

$$y_2 = -0.0017x^3+0.0984x^2-1.2661x+15.3509$$

We will further study on the solution of Al_2O_3 in low temperature aluminum electrolyte and discover impact of the additives, temperature, agitation and other factors on the dissolution of alumina by the novel method.

Acknowledgements

The authors wound like to thank reviewers for their helpful suggests. The authors wound like to thank Dr. Gang Zhang of Shenyang University of Technology for participating in simulation of algorithm. The authors also wish to thank Professor Zhaowen Wang, Dr. Xianwei Hu and students from the molten salt electrolysis research group of Northeastern University for their help. The authors wound like to acknowledge the financial supported by "National Natural Science Foundation of China (51072121)" and "Key Laboratory Foundation of Liaoning Province (LS2010109)".

References

1. Pomiakov (Поляков) et al., "Method of aluminum production: Russia", 1708933-A1 [P], 1989-06-12
2. Beck T. R., "A non-consumable metal anode for production of aluminum with low-temperature fluoride melts", Light Metals 1995, The Minerals, Metals & Materials Soc, Warrendale, USA, 1995: 355-360
3. Rolseth S., Gudbrandsen H., et al., "Low temperature aluminum electrolysis in a high density electrolyte", Aluminum, 2005, 81(5): 448-450
4. Qiu Zhuxian, Gao Bingliang, "Aluminum electrolysis in a 200A bench-scale cell at 845℃ with 96%～98% current efficiency", Aluminum, 2001, 77(12): 974-976
5. Lu H., Fang K., et al., "A new electrolytic aluminum production process", Aluminum, 1999, 75(12): 1113-1118
6. Gerlach J., Hennig U., Kern K., "The dissolution of aluminum oxide in cryolite melts", Metallurgical transactions B, 1975, 6B(3): 83-86
7. Yunshu Zhang, Xiaoxia Wu, Robert A. R., "Solubility of alumina in cryolite melts: measurements and modeling at 1300K", Metallurgical and materials transactions B, 2003, 34B(4): 235-242
8. Solheim A., Rolseth S., Skybakmoen E. et al., "Liquidus temperature and alumina solubility in the system Na3AlF6-AlF3-LiF-CaF2-MgF2", Light Metals 1995, The Minerals, Metals & Materials Soc, Warrendale, USA, 1995: 451-456
9. Egil Skybakmoen, Asbjorn Solheim, Asmund Sterten, "Alumina solubility in molten salt systems of interest for aluminum electrolysis and related phase diagram data", Metallurgical and materials transactions B, 1997, 28B(2): 81-86
10. Welch B. J., Gerda I. K., "Crust and alumina powder dissolution in aluminum smelting electrolytes", JOM, 2007, 59(5): 50-54
11. Yang Zhenhai, Gao Bingliang, Xu Ning, Qiu Zhuxain, Liu Yaokuan, "Dissolution of Alumina in Molten Cryolite: A Video Recording Study", Journal of Northeastern University (Natural Science), 1999, 20(4): 398-400
12. XU Junli , SHI Zhongning , GAO Bingliang, QIU Zhuxian, "Dissolution of Alumina in Molten Cryolite", Journal of Northeastern University (Natural Science), 2003, 24(9): 832-834
13. QIU Zhuxian, WANG Zhaowen, GAO Bingliang, YU Xuguang. Physical and chemical processes of low temperature aluminum electrolysis [J]. Mining Research and Development, 2003, 8: 9-12.

14. FAN liman, QIU Zhuxian, Grjotheim, "A direct observation of the process of aluminium in cryolite-alumina electrolyte through a transparent quartz cell", Journal of Northeastern University, 1986, 46(1): 97-106
15. XU Junli , SHI Zhongning , GAO Bingliang , QIU Zhuxian, "Bubble behavior on metal anode of aluminum electrolysis", The Chinese Journal of Nonferrous Metals, 2004, 14(2): 298-301